Design, Development and Testing of an Environmental P-T Cell for InfraRed Spectroscopy Measurements.

S. De Angelis[1], M. Ferrari[1], M.C. De Sanctis[1], D. Biondi[1], A. Boccaccini[1], A. Morbidini[1], M. Formisano[1], E. Ammannito[1-2], T. Di Iorio[1-3].

[1]IAPS-INAF (via del Fosso del Cavaliere, 100, 00133, Rome, Italy; simone.deangelis@iaps.inaf.it)

[2]ASI, Rome, Italy

[3]ENEA SSPT-PROTER-OAC, Centro Ricerche Casaccia, Via Anguillarese 301, 00123, Roma, Italy

Abstract.

Water absorption bands due to superficially adsorbed molecules often dominate the near-infrared spectra of particulate minerals and rocks, when measured in the laboratory in reflectance mode. In order to remove this spectral effect is thus necessary to acquire spectra of samples in vacuum and at higher temperatures. With the aim to accomplish this task, we developed an environmental cell to perform infrared spectroscopic measurements at controlled pressure-temperature conditions. Currently the cell allows to measuring reflectance spectra in the temperature range from room values up to 300°C (573K), in the pressure range $10^{3} \div 10^{-6}$ mbar. The acquisition of spectra continuously in two distinct phases, namely during a preliminary pumping stage (at room T) and subsequently during a heating stage (in vacuum) permits to highlight and characterize separately the effect of pressure and temperature on infrared spectra.

Introduction.

Infrared spectra of minerals and rocks acquired in the laboratory are often dominated by the presence of absorption features due to water. Minerals can contain water (H_2O) and/or have water as part of their constitutions (hydroxyl groups [OH]), or simply be surficially adsorbed water. Water in clay minerals can be strongly bound to their inner structure (i.e. bound to interlayer cations), or weakly bound externally to other water molecules through H-bond (Bishop et al., 1994). Weakly bound external water is easily removed upon heating to >100°C, while in order to remove firmly bound water, higher temperatures are needed. In the case of externally adsorbed wa-

ter due to ambient moisture and humidity, the H_2O absorption bands also occur in spectra of theoretically anhydrous minerals. Frequently, H_2O molecules coming from ambient water vapor, at standard P-T conditions, are subject to physical adsorption: the molecules quickly attach between the surface grains of the materials (especially powders, but also slabs, depending on rock texture) both during the preparation, storage and measuring phases. Fundamental absorption features due to OH-stretching and H-O-H bending transitions in water occur in the 3-6-μm spectral region, while overtones and combinations occur in the 0.9-2.5-μm region (Farmer, 1974; Clark et al., 1990). In particular, the 3-μm band consists of (i) an absorption at 2.8-3.0 μm, due to fundamental symmetric + asymmetric H_2O stretching, and (ii) an absorption at 3.1 μm, overtone of the fundamental H_2O bending at 6 μm. The 1.9-μm band consists of (i) an absorption at 1.91 μm, combination of H_2O bending + stretching, bound to cations and (ii) a second absorption at 1.95 μm, due to weakly bound water, not attached to interlayer cations (Bishop et al., 1994). Several authors have investigated the general problem of quantitatively analyzing water content of minerals and its relationship with infrared spectroscopy (e.g. Bishop & Pieters, 1995; Yen et al., 1998; Milliken, 2006), because IR spectroscopy represents a very sensitive tool for the detection of minor and trace amounts of H (in the form of H_2O molecules or hydroxyl groups) in minerals, glasses, and melts (Rossman 1988). It has been shown that the near-infrared water absorptions spectral features at 3 μm, which involve fundamental frequencies, are directly correlated with water content in the mineral. Conversely, the spectral features near 1.4 and 1.9 μm, which are overtones and combinations of O-H and H-O-H modes, are strongly dependent also on the particular mineral structure, thus do not show clear correlation with absolute water content (Milliken, 2006).

These absorptions can often mask diagnostic bands characteristic of the host materials, and this can also be problematic when using laboratory spectra for comparison and interpretation of data from planetary missions.

Numerous studies have been carried out in the past using environmental cells in order to investigate the effect of T and P on infrared spectra of samples, especially with applications to Mars surface conditions. Early infrared studies of hydrated minerals at Martian P-T laboratory conditions include the works by Bruckenthal (1987), Johnston et al. (1992). For example Bishop et al. (1994) and Bishop & Pieters (1995) studied smectites and Mars soil analogs under Martian

P-T conditions, namely at P=1 mbar in CO_2 atmosphere and at T=-40°C. Craig et al. (2006) acquired IR spectra of sulfates and other Mars analogs at low CO_2 pressure (down to $8x10^{-3}$ torr CO_2, about 10^{-2} mbar). Other authors investigated meteorites with infrared spectroscopy using P-T cells. Beck et al. (2010) and Takir et al. (2013) measured IR spectra of carbonaceous chondrites in vacuum (10^{-4}÷10^{-7} mbar) upon heating up to 200-300°C, in transmission and reflectance mode, respectively.

In this study we describe the development and testing of an environmental cell, designed to acquire infrared reflectance spectra of materials under controlled pressure and temperature. The main scientific drivers of this work have been (i) to investigate diagnostic IR absorption features in H_2O-bearing minerals, when these are masked by strong water absorptions, and (ii) to study the effect of pressure and temperature on infrared spectra of various types of minerals. The main technical motivation for developing such a custom cell was the need to couple with the SPIM facility, a VIS-IR imaging spectrometer spare of VIR onboard NASA-Dawn mission, in our laboratory (De Sanctis et al., 2011; De Angelis et al., 2015). Given the small volume available on the SPIM sampleholder, and because of small (a few cm) working distance at which the instrument focus occurs, our only choice was to realize a custom cell. Indeed the cell is small and modular, and can be easily adapted to other experimental setups in our laboratory.

Cell Design.

Requirements. The cell was designed according to specific requirements. In order to remove most of the water vapor and to avoid condensation in the sample compartment, high vacuum must be obtained within the cell. Thus the cell itself and all main parts must consist in stainless steel UHV (Ultra-High Vacuum) components. The number of inputs/outputs is limited, and all interfaces and sealing parts are ConFlat CF-components, in order to minimize vacuum losses. Interfaces apertures are foreseen in order to allow connection with the pumping system, input/output electrical transmission for temperature control and readout, cryogenic liquid flowing for sample cooling.

Mechanical-Optical design. The cell structure is an 80x80x42 mm UHV cube, manufactured by VACOM® company following our requirements (fig.1). A 3-mm thick calcium fluoride (CaF_2) window is hosted within the cell optical viewport, allowing a window of 40 mm in di-

ameter on the topside. It is characterized by a wide range of applicable viewing geometries in terms of illumination/emission angles (up to ±60° with respect to normal). The transmission spectrum of CaF_2 glass permits a good transparency from the UV up to about 8 μm. Anyway the whole cell is designed and built in a modular structure with interchangeable parts: thus the optical window can be substituted within the viewport, and different windows can be accommodated, in order to extend measurements in a different spectral range (e.g. towards the mid-IR using ZnSe or Ge glasses). The whole viewport (CaF_2 window + clamp ring flanges), designed and manufactured at INAF-IAPS mechanical workshop, can be removed in order to change the sample.

Sample-holder. The sample to be measured is placed a few millimeters below the CaF_2 window. A dedicated sample-holder was designed using SolidWorks ® 3D software and manufactured at the INAF-IAPS mechanical workshop (fig.1). The sample-holder is constituted by several layers, made of different materials, and hosts a ceramic heater that is used to warm up the sample from below. This layered structure allows most of the heat to be dissipated upward, in such a way to maximize the warming of the sample. The powdered/fragmented sample is put inside a copper cup, a few millimeters high. The cup is placed on a copper disk, 2-mm thick. The ceramic heater, which is 25.4 mm in diameter and 2.54 mm high, is tightly hosted between the copper disk above and a stainless steel ring plus a stainless steel disk below. This latter disk is sustained from below by a stainless steel piston, in order to further thermally isolate the upper part of the sample-holder from the rest of the cell. Finally the whole sample-holder is fixed on an aluminum base plate that is mounted on the bottom blank flange of the cube.

Temperature-Pressure control. In fig.2a the experimental setup is shown, while in fig.2b there is an electrical scheme. The ceramic heater made of aluminum nitride (AIN) (Ultramic Watlow®) is power supplied with 120 V_{AC} and dissipates up to 300W, it is controlled by a Solid State Relay through a Proportional–Integral–Derivative controller (PID) thermoregulator with a fast response of 0.1 s (fig.2b); this is necessary in order to control the temperature ramp of the heater which is very fast. The heater contains an integrated type K thermocouple, which is read through the PID controller, which allows the temperature to be set and measured directly below the cup. Once the temperature set point is programmed on the PID, the system takes a few minutes to reach the temperature value and to stabilize. The maximum temperature that can be reached with the current heater is about 400°C. Numerical simulations have been carried out, using COMSOL Mul-

tiphysics ®, in order to evaluate the temperature gradient along the sample-holder, and to estimate the error about the sample temperature (fig.3). The numerical simulations are based on a 3D finite element method. The developed model solves the heat equation with no convection term. A radiation condition is imposed on the boundaries of the cup. Three models have been simulated, corresponding to different temperature set points, namely: $T_{SET\text{-}POINT}$=373K, 473K and 673K respectively. In all cases the vacuum pressure is assumed, $p=10^{-5}$-10^{-6} mbar. In all cases the simulations show that the whole sample-holder reaches an equilibrium temperature within a time interval $t<10$ s, after the heater has stabilized at the fixed temperature set point. The temperature at the center of the cup becomes practically equal to the temperature set point after a few seconds. The lower part of the sample-holder, below the stainless steel ring, remains cold at about 300K in all cases. Thus we can safely assume that after waiting about 1 min for sample thermalization, the temperature error between sample and thermocouple is below 5 degrees.

The currently used pumping group consists of a primary rotary vane pump, with lower limit pressure of about 10^{-2} mbar, and a turbo-molecular pump, with current lower limit pressure of 10^{-8} mbar (fig.4). A Pirani-Penning gauge permits to measure the pressure in the room-vacuum range (fig.2a).

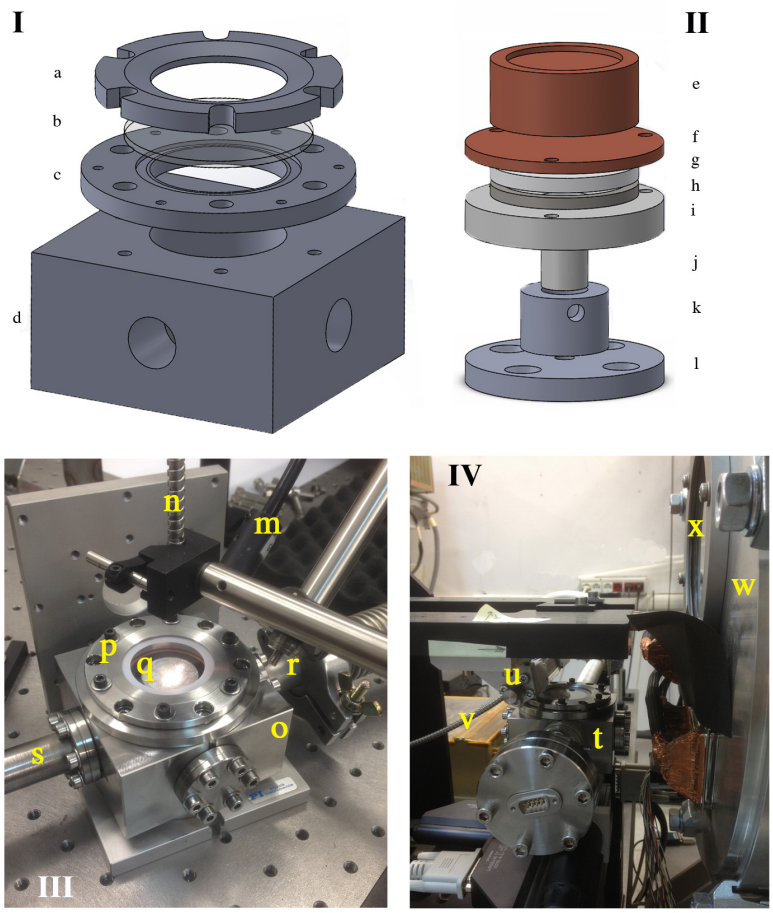

Fig.1. I. Cell and optical viewport design: a) viewport clamp ring; b) CaF_2 window; c) viewport flange; d) UHV cube. II. Sample-holder: e) copper sample holder; f) copper disk; g) ceramic AIN heater; h) stainless steel ring; i) PTFE disk; j) PTFE piston; k) aluminum cylindrical support; l) aluminum base plate. III. Cell photograph (FieldSpec Pro setup): m) QTH Light Source emitting fiber; n) FieldSpec Pro collecting fiber bundle; o) cell; p) optical viewport; q) sample (illuminated); r) pumping line; s) temperature control line. IV. Cell photograph (SPIM setup): t) cell on the sample holder; u) illumination system; v) illumination optical fiber; w) SPIM thermal vacuum chamber; x) CaF_2 window for TVC.

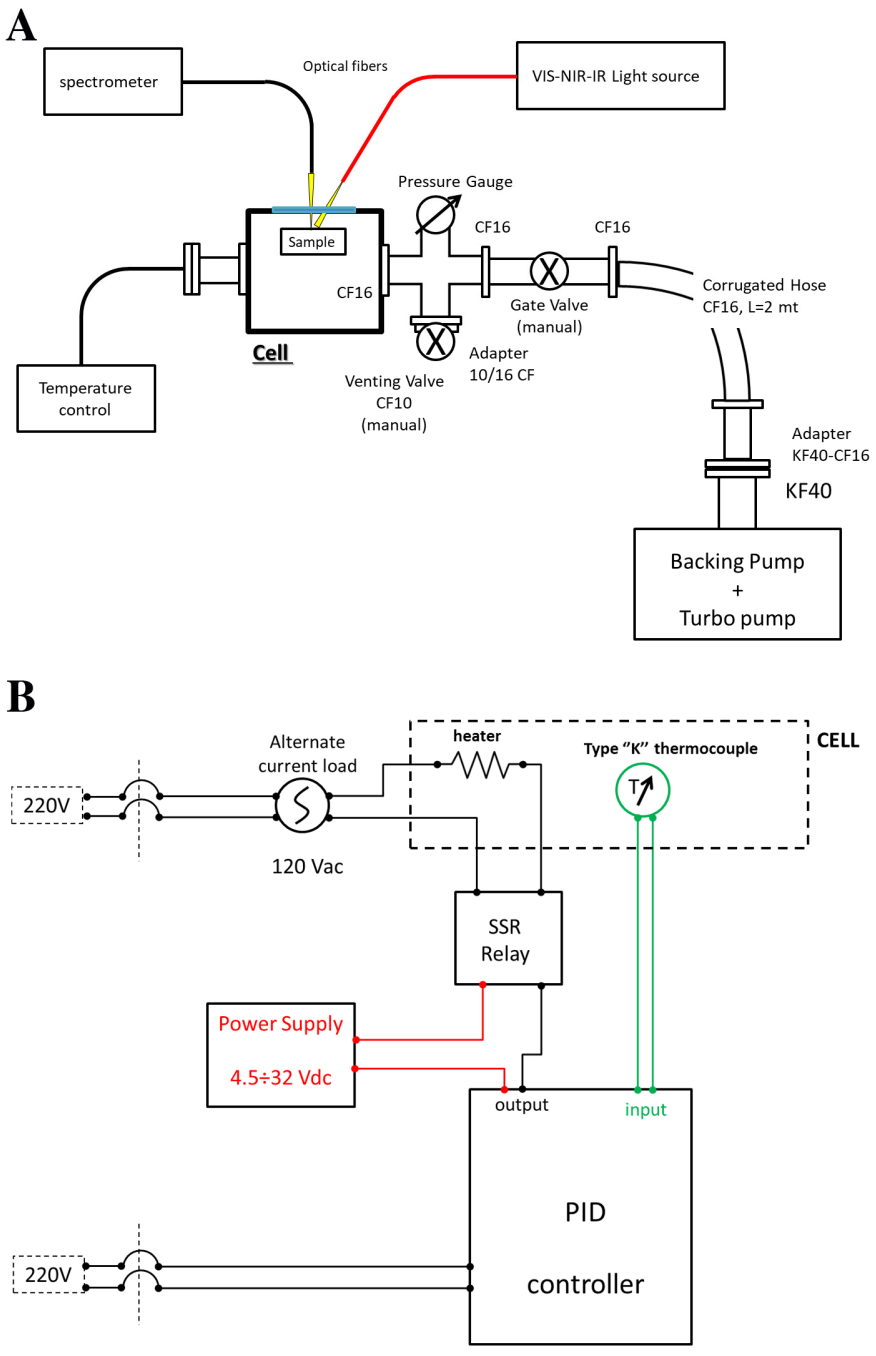

Fig.2. A: the experimental setup used to perform test measurements with the cell. Here the spectrometer is the FieldSpec Pro, the light source is a QTH lamp. B: the electrical scheme for the temperature control by means of a PID thermoregulator. The thermocouple and heater are located inside the cell.

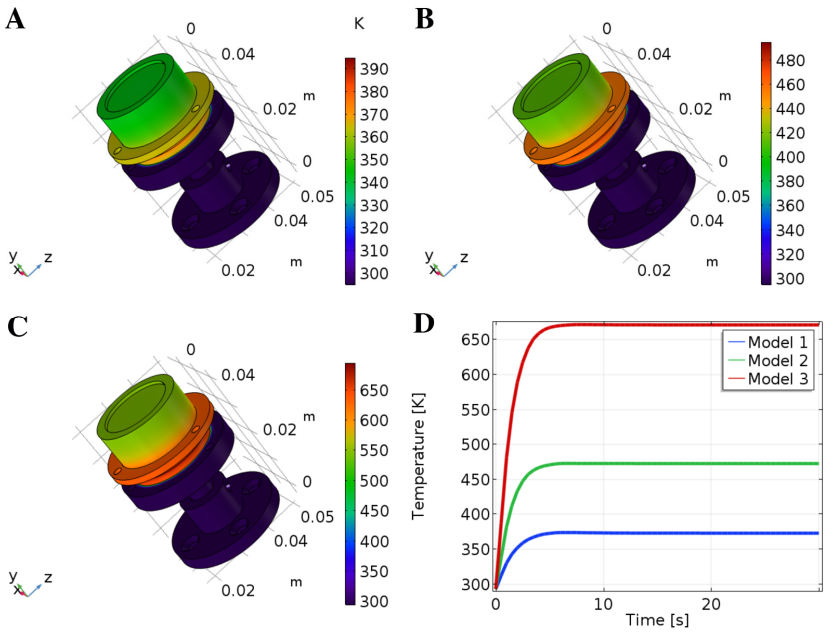

Fig.3. Numerical simulations showing the thermal behavior of the sample-holder upon heating. The thermal maps are retrieved at t=1.5 s after the heater has reached a stabilized temperature (set point). A: model 1, $T_{SET\text{-}POINT}$=373K. B: model 2, $T_{SET\text{-}POINT}$=473K. C: model 3, $T_{SET\text{-}POINT}$=673K. D: temperature versus time plot, computed at the center of the cup. For all three models, the system reaches equilibrium after t<10 s.

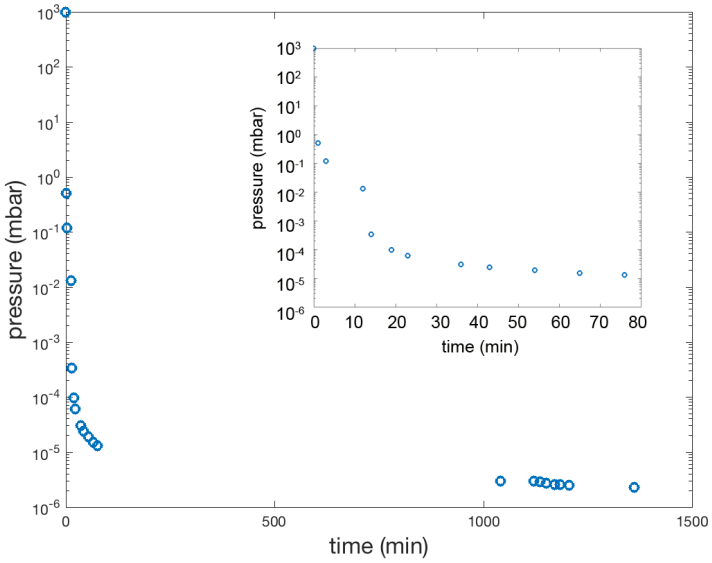

Fig.4. Vacuum level reached within the cell, in the current configuration, with rotary vane as primary pump and turbo-molecular as secondary pump.

Test setup and measurements.

Measurement procedure. We performed numerous tests with various types of powder samples, mostly phyllosilicates and other minerals with different hydration states, using a FieldSpec Pro spectro-photometer in the range 0.35-2.5 μm and a 100W QTH lamp. The test setup in depicted in fig.2a. Test measurements in the 1.5-5 μm range were carried out coupling the cell with the SPIM imaging spectrometer facility (De Angelis et al., 2015). The measurement procedure we followed in order to carry out acquisitions consists of a sequence of steps.

In the first stage we acquire the room P-T spectrum of the standard reference target, outside the cell, which is a Labsphere Spectralon, at T=298 K and P=10^3 mbar. Then the first spectrum of the sample is acquired at room P-T. Subsequently the pumping group is switched on and during the whole pumping phase numerous reflectance spectra are consecutively acquired in continuously running mode, while the pressure drops down. Although the vacuum limit pressure of the turbomolecular pump is about 10^{-8} mbar, the actual value of the limit pressure reached inside the cell, before starting the heating phase, is evaluated according to the starting hydration state of the sample. Once the pressure starts to decrease, degassing and water desorption begins from the sample grains, thus limiting the achievable vacuum. When measuring heavily hydrated materials, an inversion in pressure values can occur at a few mbar, that is when the pressure drops below the water vapor pressure at room temperature (about 20 mbar at 20°C). The primary membrane pump alone is used until again an inversion occurs and the pressure restarts to decrease, then the turbomolecular pump is switched on.

Once the limit pressure is reached with the turbomolecular pump and a stationary high vacuum is present within the cell (P=10^{-4}÷10^{-5} mbar), we start to acquire spectra at different temperatures. Sample spectra are acquired typically at temperature steps of about 25-50°C in the range 25÷300°C. After the temperature set point is fixed on the PID, we wait until the sample-holder has reached the desired temperature and stabilized, before to start the acquisition. The PID controller allows the heater to reach the set point temperature very fast, a few seconds for temperatures below 100°C, and a few minutes as the temperature set point increases towards 300°C. The stabilization time for the sample-holder is very short, as discussed in the previous section. For most tested samples, a great amount of adsorbed water is lost during pumping down to high vacuum, and then upon heating up to 150-200°C. Below this temperature most of hydrated minerals

(e.g. phyllosilicates) still preserve their unaltered structure, in accordance with the literature Thermo Gravimetric Analyses (TGA) data.

Example 1. Hydrated mineral: kaolinite.

Measurement in pumping stage. A kaolinite powder sample (particles size <50 μm) (Kln_G, with empirical formula $Al_{2.01}Si_{2.00}O_5(OH)_4$, Ferrari et al., 2014) was measured as a first example of slightly hydrated mineral. The spectra of kaolinite acquired during the initial pumping phase from 10^3 down to 10^{-4} mbar are shown in figure 5a. The spectrum acquired on the raw sample is characterized by two deep absorptions near 1.4 and 1.9 μm, due to vibrational transitions in OH and H_2O respectively (Clark et al., 1990). The narrow band near 2.2 μm is due to vibrational transitions in X-OH bonds, likely Al-OH stretching (Clark et al., 1990). Two weak artifacts occur at 1.1 and 1.3 μm, and are related to a reflection contribution from the CaF_2 window. During the pumping in the $10^3 \div 10^{-4}$-mbar pressure range, the OH/H_2O bands due to physically adsorbed water undergo a decrease in both depth and width. The relatively broad band at 1.4 μm (Fig. 5b), appears to be composed by three close absorptions.

Bands positioned at shorter wavelengths 1.36 and ~1.40 μm are attributed to hydrogen-bonded OH groups located on the exterior surfaces of the octahedral sheets, whereas the band at longer wavelengths ~1.415 μm is produced by the inner hydroxyl groups (Crowley and Vergo, 1988). All these OH-related bands decrease during the pumping phase with the decreasing of pressure (fig.5b). Likewise, the 1.9-μm (fig. 5c) water band decreases by more than 80%, whereas the Al-OH band at ~2.2 μm seems to be not affected by the pumping, because characterized by stronger bonds.

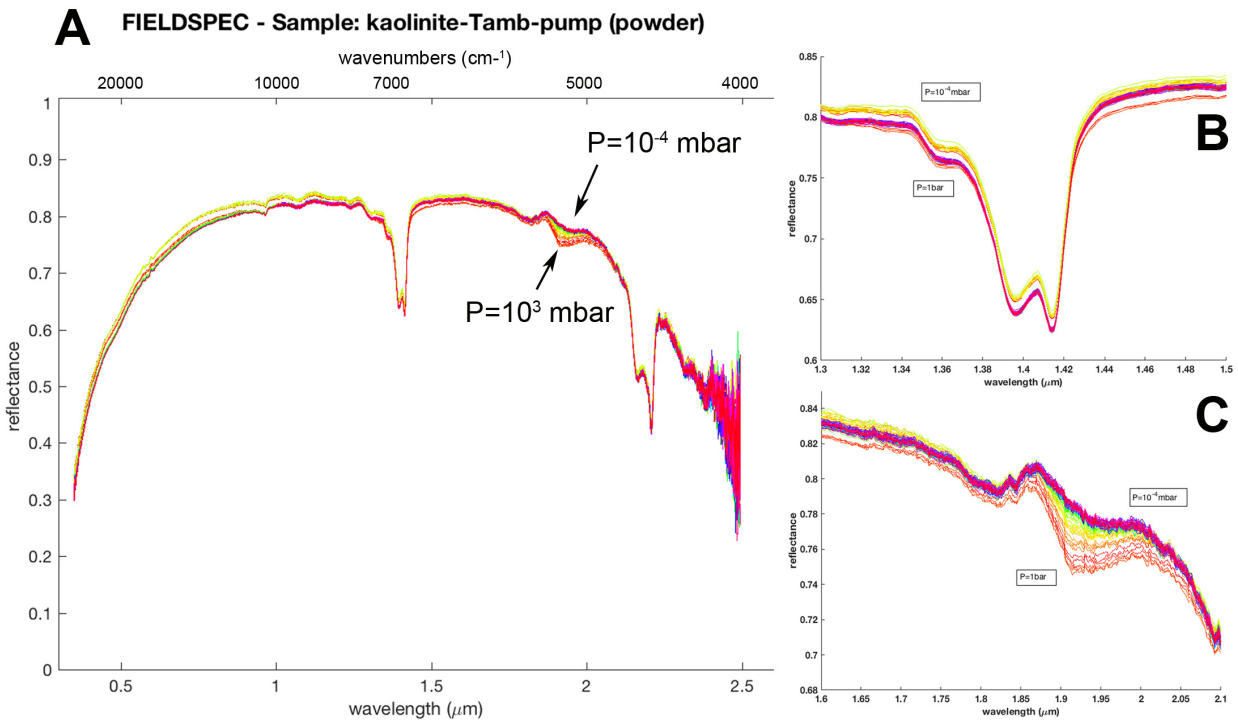

Fig.5. Spectra of kaolinite acquired with FieldSpec Pro during the pumping phase from 10^3 to 10^{-4} mbar: a) full range spectra; b) the 1.4 µm absorption band; c) the water absorptions at 1.9 µm almost disappear during the pumping. Wavenumbers (cm^{-1} units) are reported as secondary axis in panel A.

Measurement in heating stage. In this stage the stationary vacuum is reached in the cell (about P=10^{-4}-10^{-5} mbar) and spectra are acquired at different temperatures. Temperature steps of 15-25°C have been performed in the 50÷300°C range. The spectra of heated kaolinite are shown in figure 6. The initial spectrum acquired at room P-T conditions (1 bar, 25°C) is shown for comparison (red line). Heating spectra are characterized by a further decreasing of OH and H_2O bands at 1.4 and 1.9 µm as the temperature raises, as well as by red slope in the IR side (because of increasing thermal emission). At 225°C the 1.9-µm absorption band has reduced by about 90%, and the 1.4-µm triplet feature further decreases. For temperatures >240°C the Al-OH feature at ~ 2.2 µm is largely reduced, even if the dehydroxylation temperature was not reached.

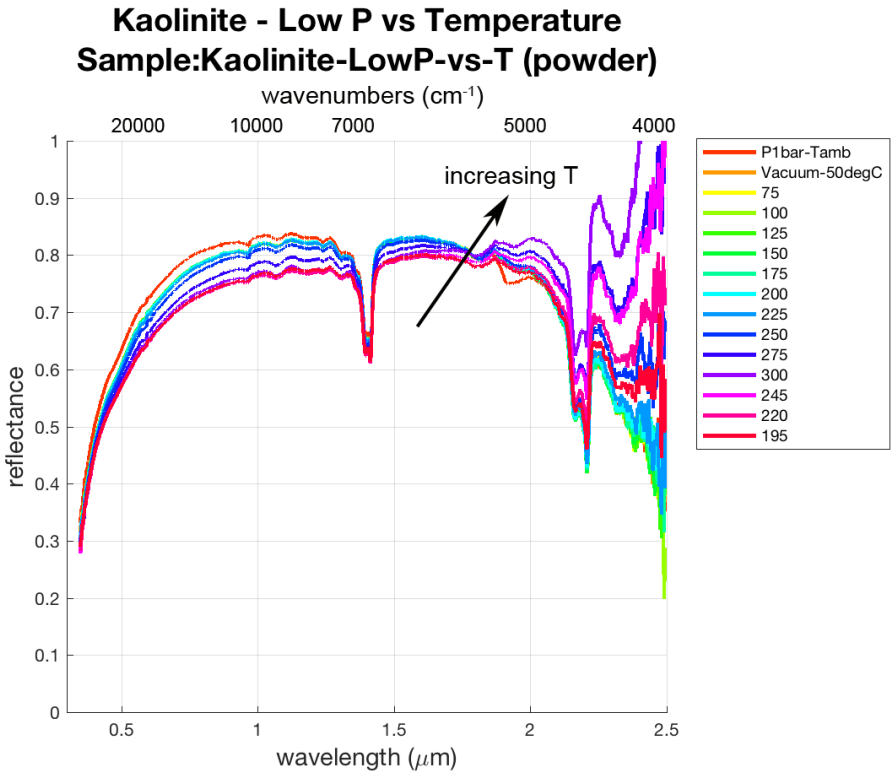

Fig.6. Spectra of kaolinite acquired with FieldSpec Pro in vacuum, during the heating phase. The starting spectrum (room P-1 bar-Tamb) is reported for comparison. Spectra are acquired during the temperature ramp 50-300 °C; the violet spectrum is at highest temperature (300°C). Further spectra were acquired after stopping the heating, during the slow cooling of the sample (245, 220 and 195°C spectra). Wavenumbers (cm^{-1} units) are reported as secondary horizontal axis.

Example 2. Anhydrous mineral: Enstatite.

As a second example we considered an anhydrous mineral, enstatite (ENST1). The measurement procedure that we followed in this case is the same as described previously. In fig.7a the spectra acquired during the pumping phase are shown. In the case of enstatite the absorption bands are characterized by a quite different behavior. The band at 1 μm, due to crystal field electronic transition in Fe^{2+} (Burns, 1993), does not show any appreciable dependence on pressure. The band at 2 μm, instead, is characterized by a slight decrease in depth. This band is actually composed by the crystal field absorption in Fe^{2+}, which is independent of ambient pressure in this range, and the water absorption at 1.9 μm (fig.7b), which clearly decreases during the pump-

ing in the range 10^{3}÷10^{-4} mbar. The other two bands near 1.4 and 2.3 μm are related to OH and Mg-OH respectively, likely due to some degree of hydration in enstatite and not strongly dependent on pumping.

In the second stage, upon heating in the range 60÷280°C, the spectra of enstatite show a notable variation in dependence of temperature (fig.8). The 1-μm band is characterized by an evident broadening with increasing temperature. The 2-μm band is subject to a decreasing of depth mainly due to water removal. Above 200°C a dramatic increase in the continuum towards longer wavelengths is due to thermal emission, which for example for the 280°C-spectrum peaks at 5 μm.

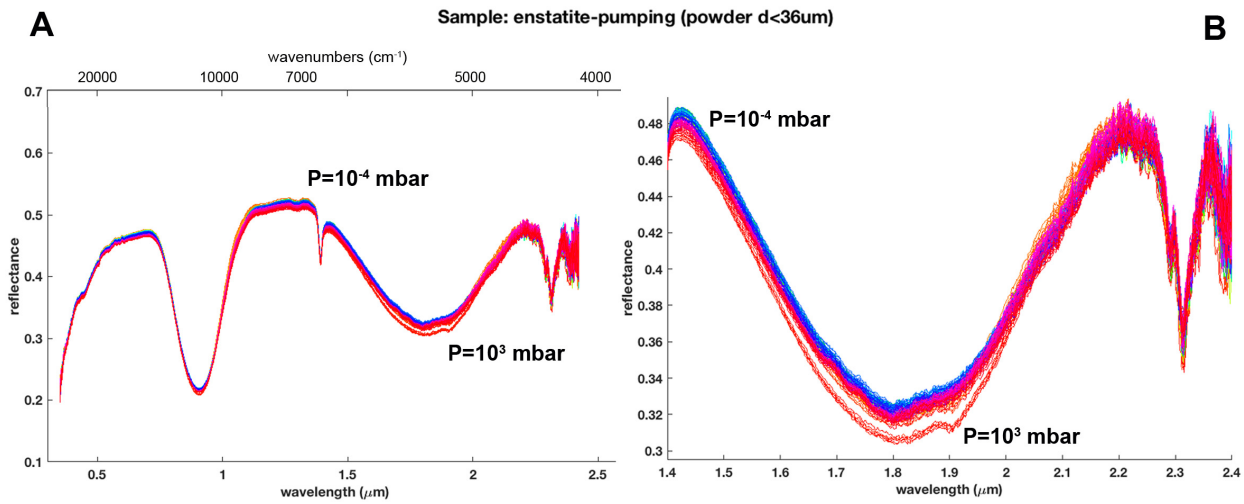

Fig.7. Spectra of enstatite, acquired with FieldSpec Pro during the pumping phase, from 10^{3} to 10^{-4} mbar. Wavenumbers (cm^{-1} units) are reported in panel A as secondary horizontal axis.

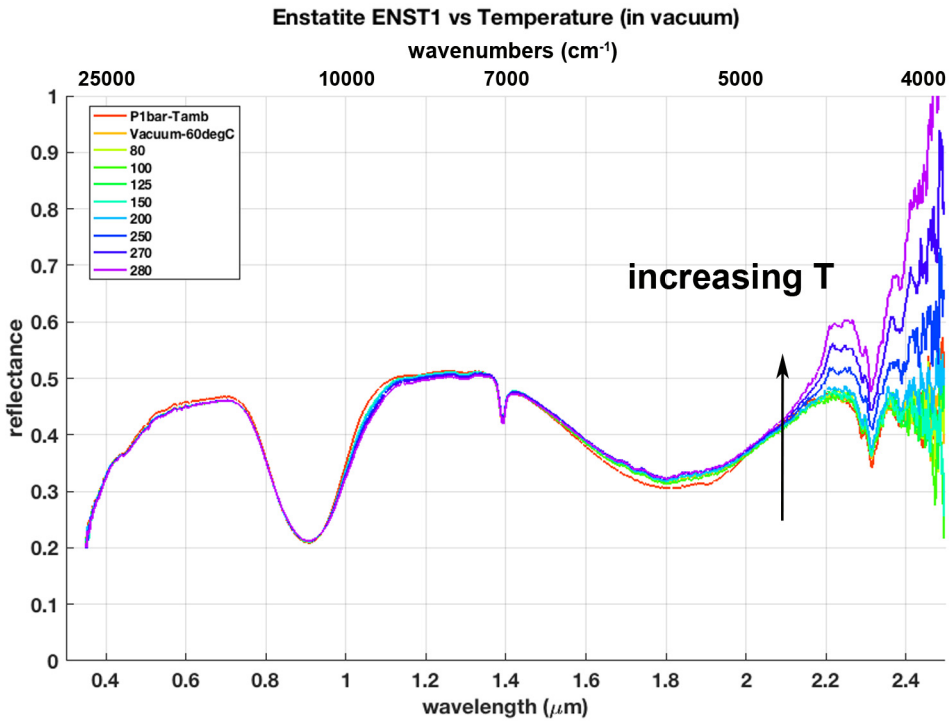

Fig.8. Spectra of enstatite acquired with FieldSpec Pro in vacuum, during the heating phase. The starting spectrum (room P-T) is in red, for comparison. Spectra are acquired during the temperature ramp 60-280 °C. Wavenumbers (cm^{-1} units) are reported as secondary horizontal axis.

Example 3. Thenardite / Sodium sulfate (1.5-5 μm).

As further test we used thenardite (sodium sulfate, Na_2SO_4, fig.9). We acquired reflectance spectra of a powder sample by means of the SPIM facility spectrometer (De Angelis et al., 2015) in the range 1.5-5 μm, following the same procedure as in the previous tests: (i) sequential acquisitions at room temperature, and pressure varying from 10^3 down to 10^{-4} mbar; (ii) acquisitions at increasing temperatures, in vacuum. In fig.9 the spectra are shown. The room P-T spectrum (blue diamonds) shows hydration features: although the sodium sulfate is nominally anhydrous, a small amount of adsorbed water was present on the sample, as evidenced by the absorption band at 3 μm, due to hydration of the sample powder during storage, preparation and measurement. In the spectrum acquired at room temperature in vacuum (green squares) the 3-μm water band is somewhat decreased. Finally in the spectrum acquired in vacuum and at T=200°C (red crosses) the 3-μm hydration feature is largely reduced. Secondary minima occurring near 3.1, 3.2 and 3.4 μm are likely due to some organics present in the sample in minor amounts, while the broad

band near 4.5 μm is related to sulfate. Here the continuum background affects the band shape; in particular in the 200°C-spectrum the thermal emission strongly affects the spectral slope (reddening). In fig.10 spectra with continuum removed are shown. The continuum background was taken as a straight line between 2.6-3.6 μm and then removed by division by each spectrum. The changing of 3-μm water band with pressure and temperature then appears clearer when looking at continuum removed spectra.

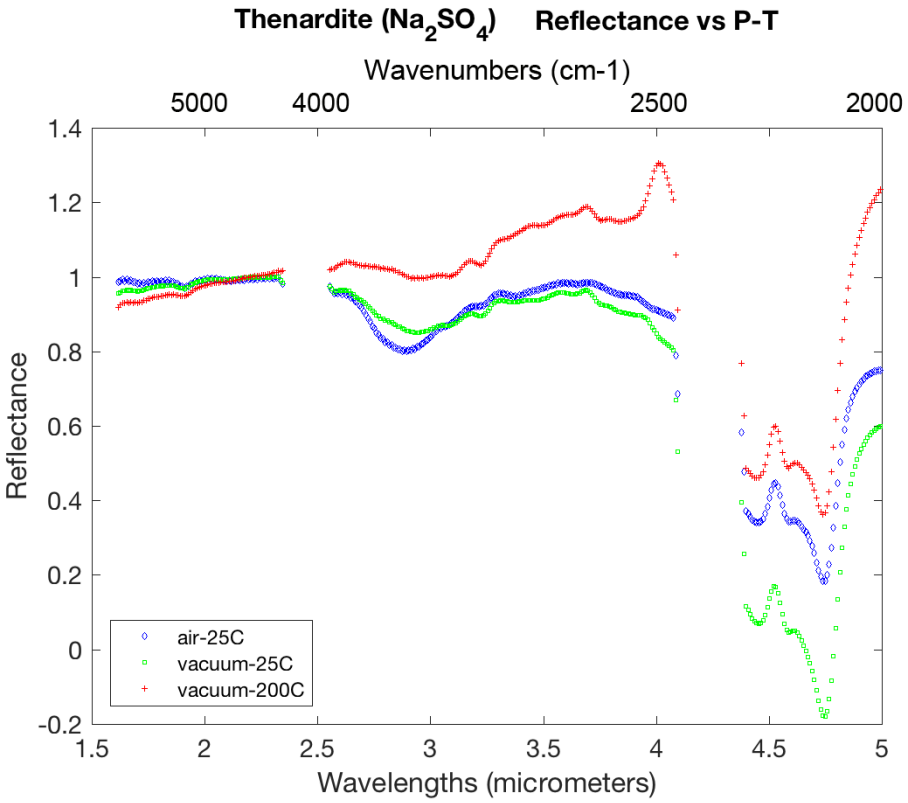

Fig.9. Spectra of thenardite (sodium sulfate) acquired with the Spectral Imaging facility in the 1.5-5 μm range. Blue diamonds: ambient pressure (10^3 mbar) and temperature (25°C). Green squares: vacuum (10^{-4} mbar) and ambient temperature. Red crosses: vacuum and T=200°C. Wavenumbers (cm^{-1} units) are reported as secondary horizontal axis.

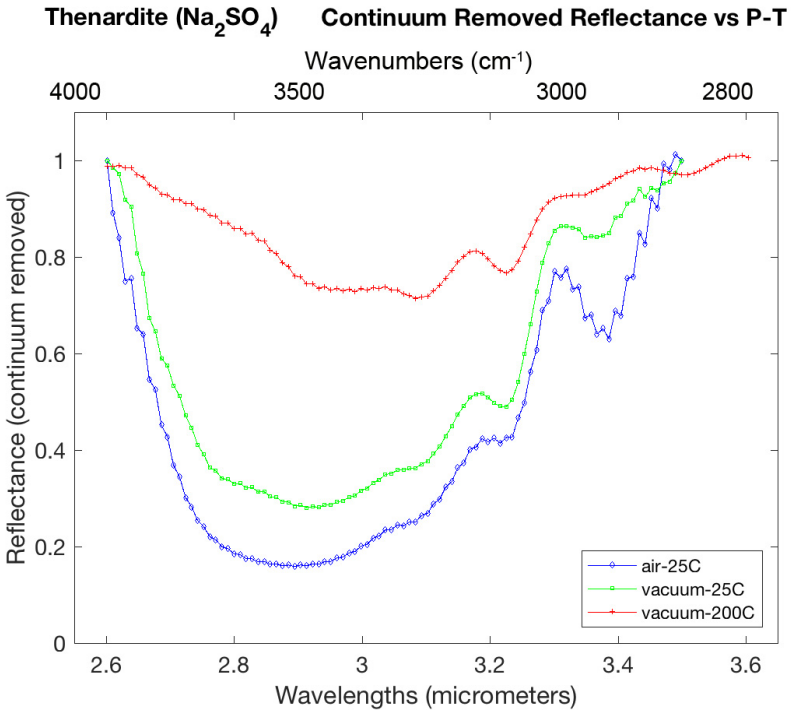

Fig.10. Spectra of thenardite (sodium sulfate) acquired with the Spectral Imaging facility in the 1.5-5 μm: continuum removed reflectance in the 3 μm region (water absorption). Wavenumbers (cm^{-1} units) are reported as secondary horizontal axis.

Conclusions and future work

We developed a custom environmental cell with the aim to perform visible-infrared reflectance spectroscopy measurements in numerous different conditions of pressure and temperature and in a broad spectral range from the visible to the mid-infrared. The reduced size of the cell indeed makes it to be used with different instruments. In the current configuration the cell allows measurements to be performed in a range of pressures between $10^{3} \div 10^{-6}$ mbar and in the range of temperatures from room up to 300°C. The test performed in the spectral range 0.3-5.1 μm showed clearly the reduction of hydration spectral features experienced by the samples with varying pressure and temperature. Future work is ongoing in order to upgrade the cell, with the aim to extend the possibility to acquire spectra also at cold temperatures. This cell is a valuable mean for the investigation of the spectral behavior of samples (minerals, rocks, meteorites) in a broad range of pressure and temperatures. Reflectance spectral data produced at different laboratory P-

T conditions will be useful in the future for the understanding and interpretation of data from planetary missions.

Acknowledgements

This work is supported by the Italian Space Agency.

References:

Beck P., E. Quirico, G. Montes-Hernandez, L. Bonal, J. Bollard, F.-R. Orthous-Daunay, K.T. Howard, B. Schmitt, O. Brissaud, F. Deschamps, B. Wunder, S. Guillot: *Hydrous mineralogy of CM and CI chondrites from infrared spectroscopy and their relationship with low albedo Asteroids*, Geochimica et Cosmochimica Acta 74, 4881–4892, 2010

Bishop J.L., Pieters C.M. and Edwards J.O.: *Infrared Spectroscopic Analyses on the Nature of Water in Montmorillonite*, Clays and Clay Minerals, vol.42, N.6, 702-716, 1994

Bishop J.L. and Pieters C.M.: *Low-temperature and low atmospheric pressure infrared reflectance spectroscopy of Mars soil analog materials*, Journal Of Geophysical Research, Vol. 100, No. E3, Pages 5369-5379, 1995

Bruckenthal, E. A., *The dehydration of phyllosilicates and palagonites: Reflectance spectroscopy and differential scanning calorimetry*, M.S. thesis, Univ. of Hawaii, Honolulu, 1987

Burns C., *Mineralogical applications of Crystal Field Theory*, ISBN 9780511524899, (Cambridge Topics in Mineral Physics and Chemistry, pp. I-Vi). Cambridge: Cambridge University Press, 1993

Clark, R.N., et al: *High spectral resolution reflectance spectroscopy of minerals*. Journal of Geophysical Research 95 (B8), 12653–12680, 1990

Craig M., E. A. Cloutis, L. Kaletzke, K. McCormack, and L. Stewart: *Alteration Of Hydration Absorption Features In Reflectance Spectra Of Selected Sulfates In A Low Pressure Environment: 0.45-4.3 μm*, Lunar and Planetary Science XXXVII, LPSC abstract n.2112, 2006

Crowley J. K. and Vergo N. *Near-Infrared Reflectance Spectra of Mixtures of Kaolin-Group Minerals*: Use in Clay Mineral Studies . 1988 Clays and Clay Minerals. v. 36; no. 4; p. 310-316; DOI: 10.1346/CCMN.1988.0360404

De Angelis S., Ammannito E., Di Iorio T., De Sanctis M.C., Manzari P.O., Liberati F., Tarchi F., Dami M., Olivieri M., Pompei C., and Mugnuolo R.: *The spectral imaging facility: setup characterization*, Review of Scientific Instruments, 86, 093101, http://dx.doi.org/10.1063/1.4929433, 2015

M.C. De Sanctis, A. Coradini, E. Ammannito, G. Filacchione, M.T. Capria, S. Fonte, G. Magni, A. Barbis, A. Bini, M. Dami, I. Ficai-Veltroni, G. Preti, VIR Team: *The VIR spectrometer*, Space Sci Rev, 163:329–369 DOI 10.1007/s11214-010-9668-5, 2011

Farmer, V. C.: *The vibrations of protons in minerals: hydroxyl, water, and ammonium*, in *The infrared spectra of minerals*, edited by V. C. Farmer, pp. 137-181, Mineralogical Society, London, 1974.

Ferrari, M., Della Corte, V., Rotundi, A., Rietmeijer, F.J.M.: *Single minerals, carbon-and ice-coated single minerals for calibration of GIADA onboard ROSETTA to comet 67P/Churyumov-Gerasimenko*. Planetary and Space Science. 101, 53–64. doi:10.1016/j.pss.2014.06.006, 2014

Johnston, C. T., Sposito, G., Erickson C.: *Vibrational probe studies of water interactions with montmorillonite*, Clays Clay Miner., 40, 722 – 730, 1992

Milliken PhD Thesis, *Estimating the Water Content of Geologic Materials Using Near-Infrared Reflectance Spectroscopy: Applications to Laboratory and Spacecraft Data*, PhD Thesis, 2006

Rossman, G.R.: *Vibrational Spectroscopy of hydrous components*. In Mineralogical Society of America Reviews in Mineralogy, 18, 193– 206, 1988

Takir D., Emery J.P., McSween H.Y.Jr., Hibbitts C.A., Clark R.N., Pearson N., and Wang A.: *Nature and degree of aqueous alteration in CM and CI carbonaceous chondrites*, Meteoritics & Planetary Science 48, Nr 9, 1618–1637, doi: 10.1111/maps.12171, 2013

Yen A.S., Murray B.C. and Rossman G.R.: *Water content of the Martian soil: Laboratory simulations of reflectance spectra*, Journal of Geophysical Research, vol.103, N.E5, pp.11,125-11,133, 1998

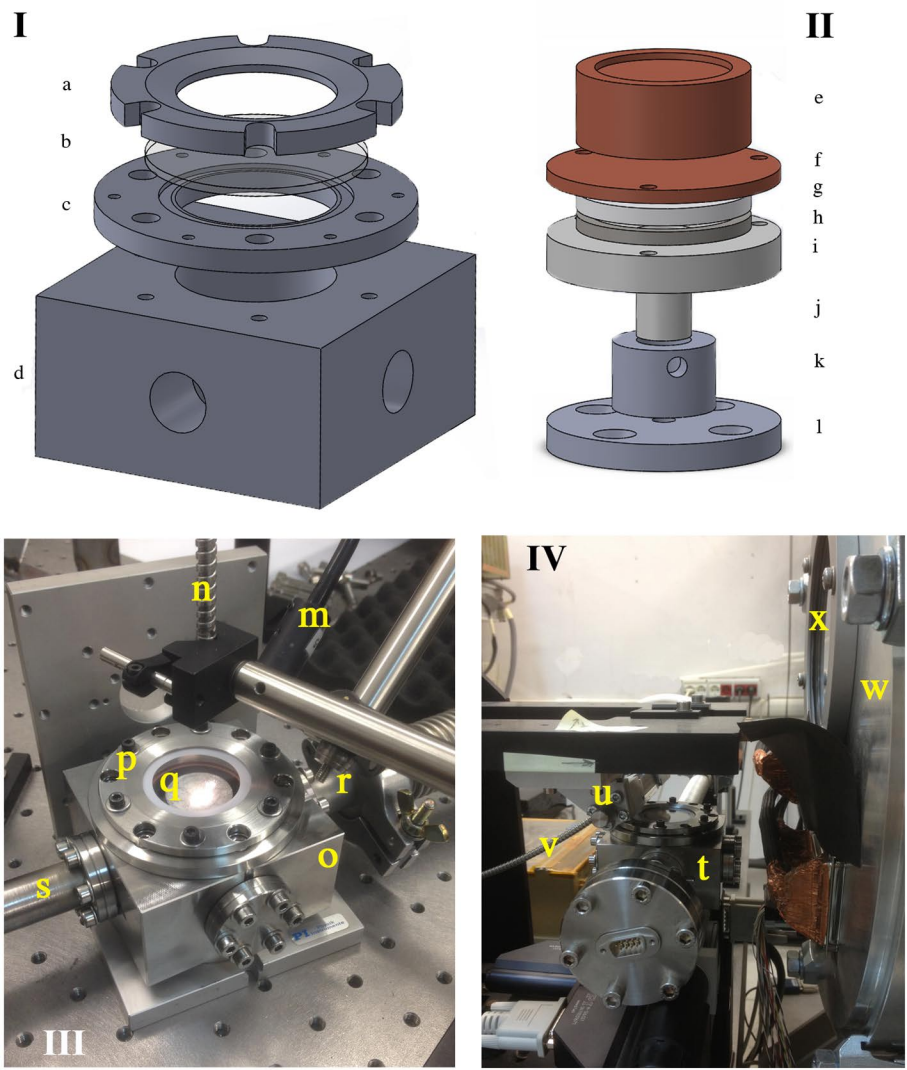
I
a
b
c
d
II
e
f
g
h
i
j
k
l
III
n
m
p
q
r
o
s
IV
x
w
u
v
t

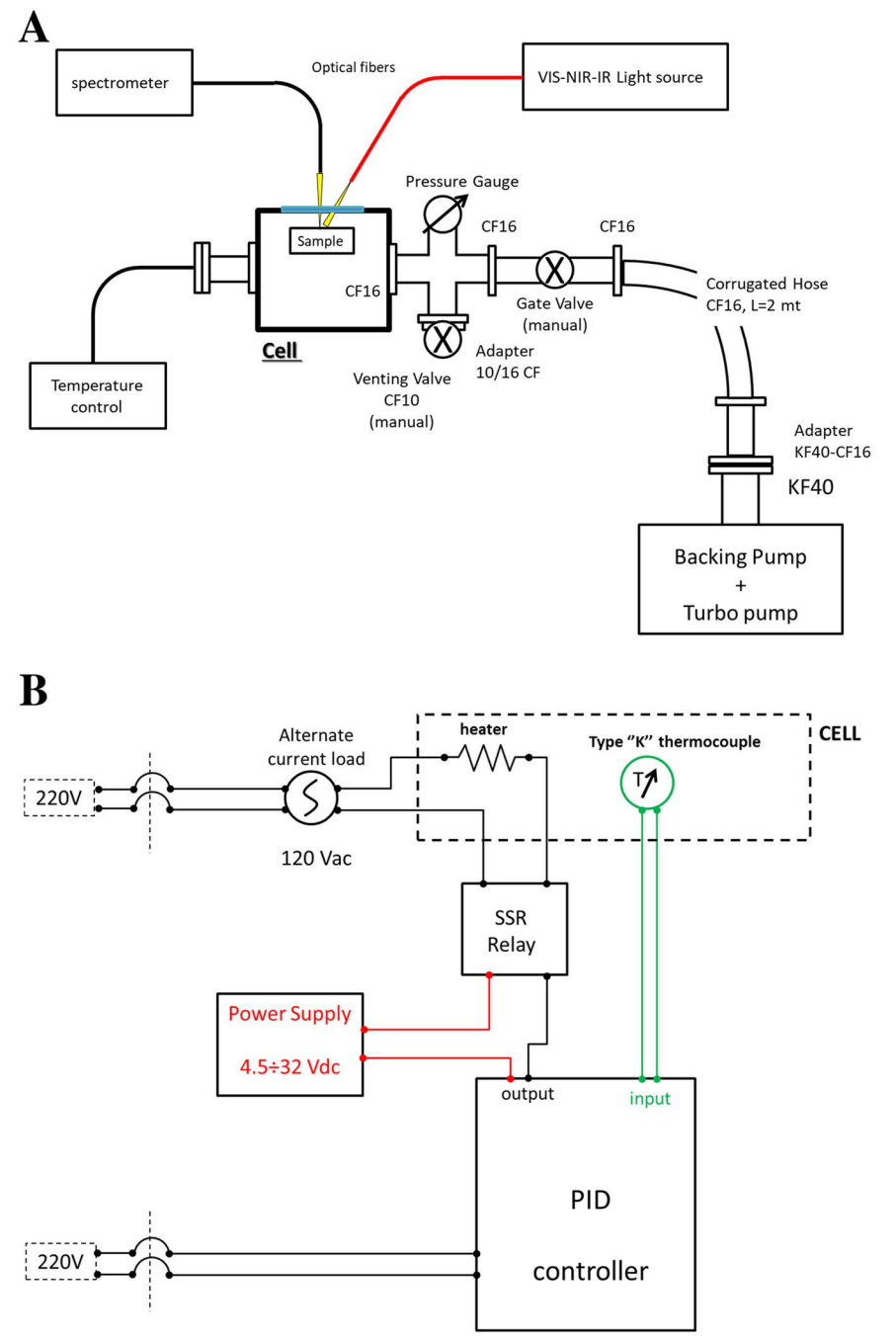
A
spectrometer
Optical fibers
VIS-NIR-IR Light source
Pressure Gauge
Sample
CF16
CF16
CF16
Gate Valve
(manual)
Corrugated Hose
CF16, L=2 mt
Cell
Temperature
control
Venting Valve
CF10
(manual)
Adapter
10/16 CF
Adapter
KF40-CF16
KF40
Backing Pump
+
Turbo pump
B
Alternate
current load
heater
Type "K" thermocouple
CELL
220V
120 Vac
SSR
Relay
Power Supply
4.5÷32 Vdc
output
input
PID
controller
220V

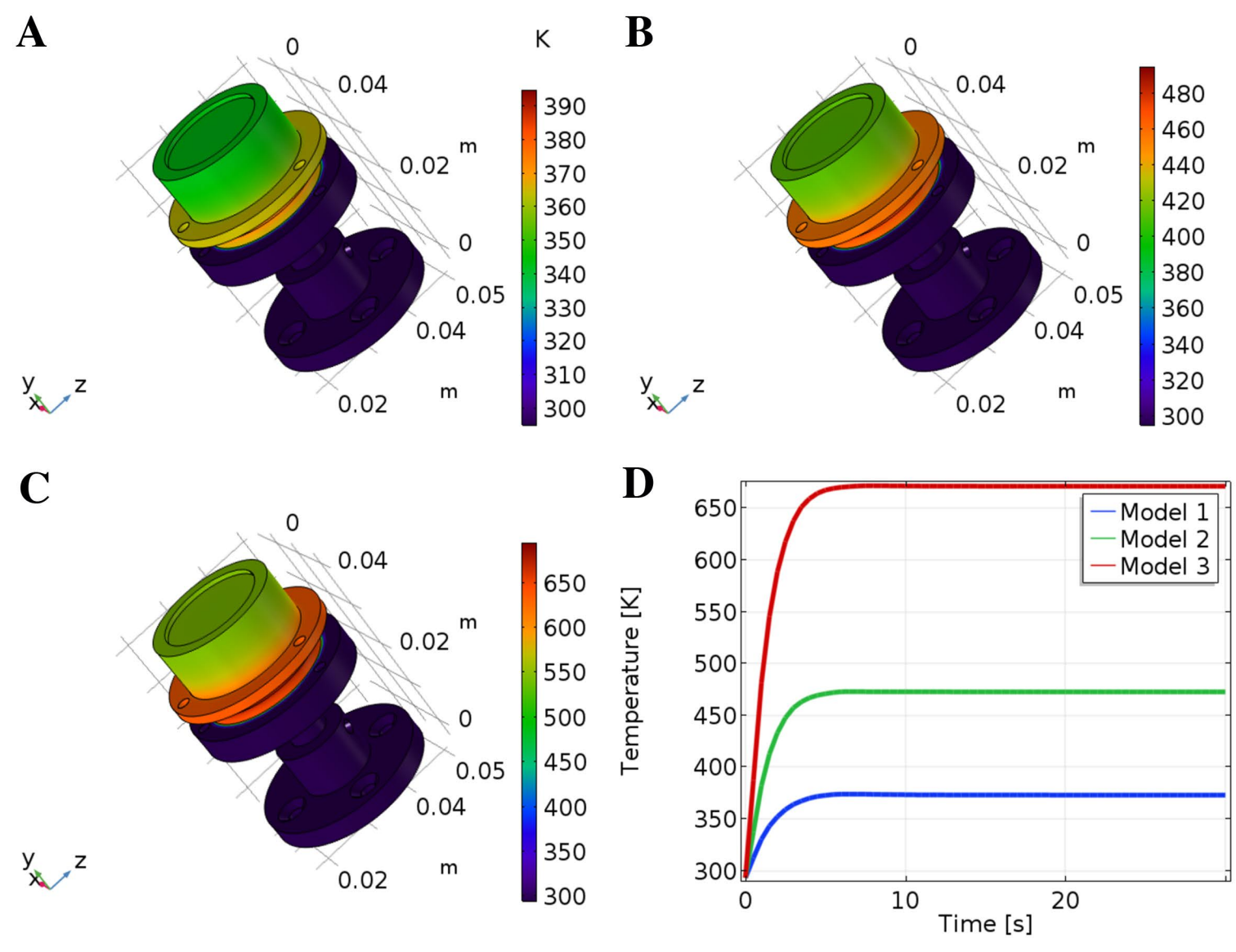
A
K
390
380
370
360
350
340
330
320
310
300
0
0.04
0.02
m
0
0.05
0.04
0.02
m
y
z
x
B
480
460
440
420
400
380
360
340
320
300
C
650
600
550
500
450
400
350
300
D
Model 1
Model 2
Model 3
Temperature [K]
Time [s]
0
10
20

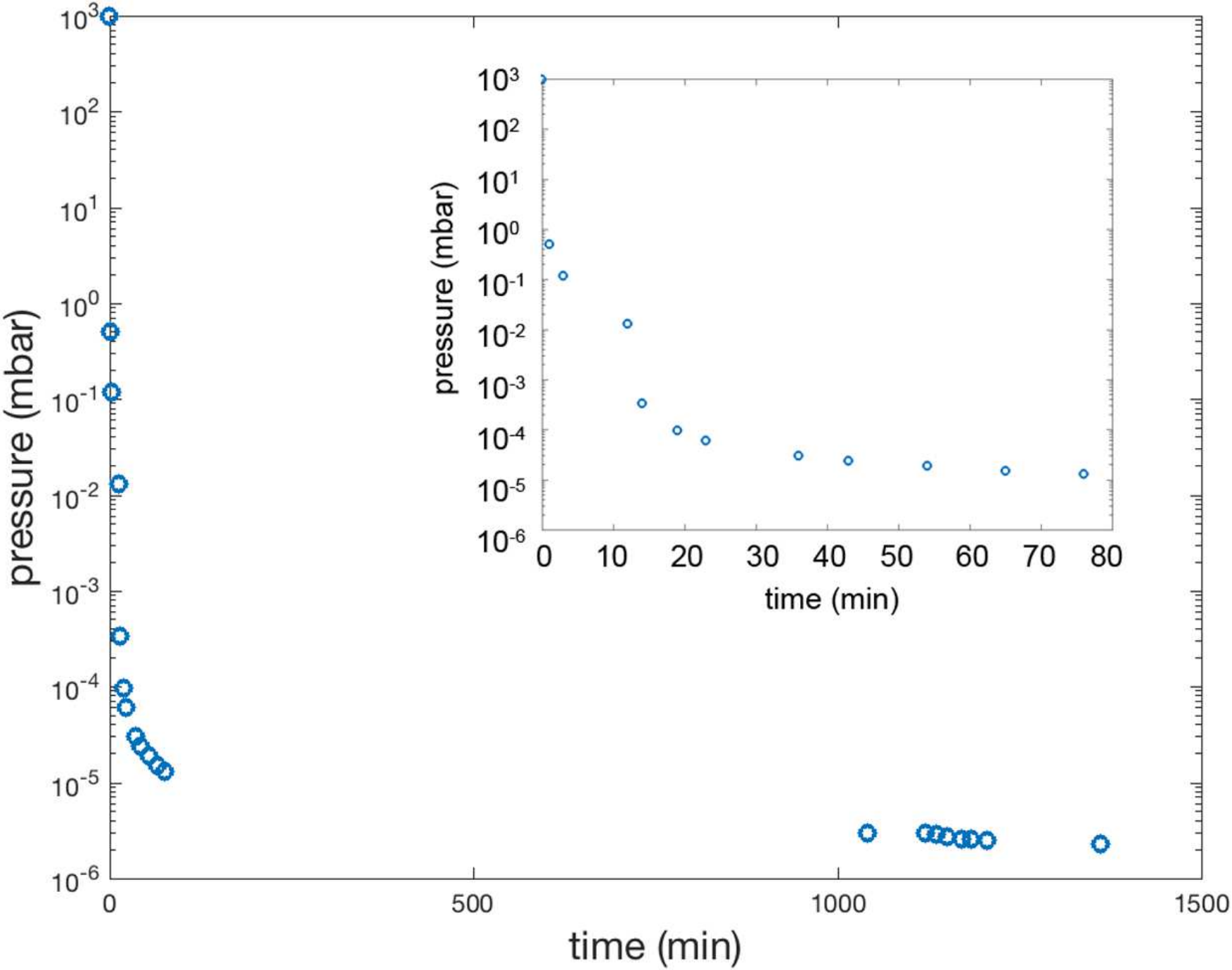
pressure (mbar)
time (min)
pressure (mbar)
time (min)

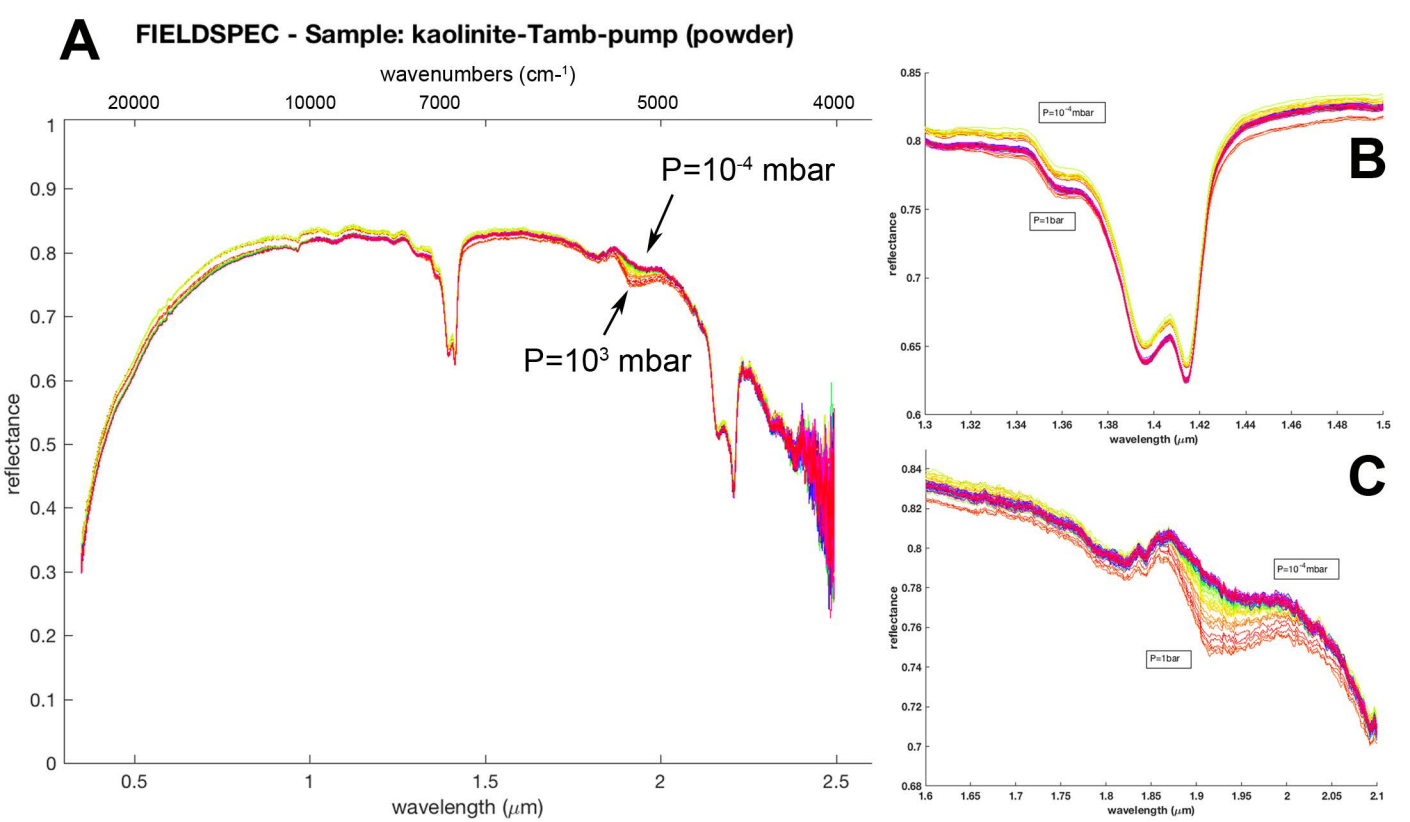
A
FIELDSPEC - Sample: kaolinite-Tamb-pump (powder)
wavenumbers (cm-1)
20000
10000
7000
5000
4000
P=10-4 mbar
P=103 mbar
reflectance
wavelength (μm)
B
P=10-4mbar
P=1bar
reflectance
wavelength (μm)
C
P=10-4mbar
P=1bar
reflectance
wavelength (μm)

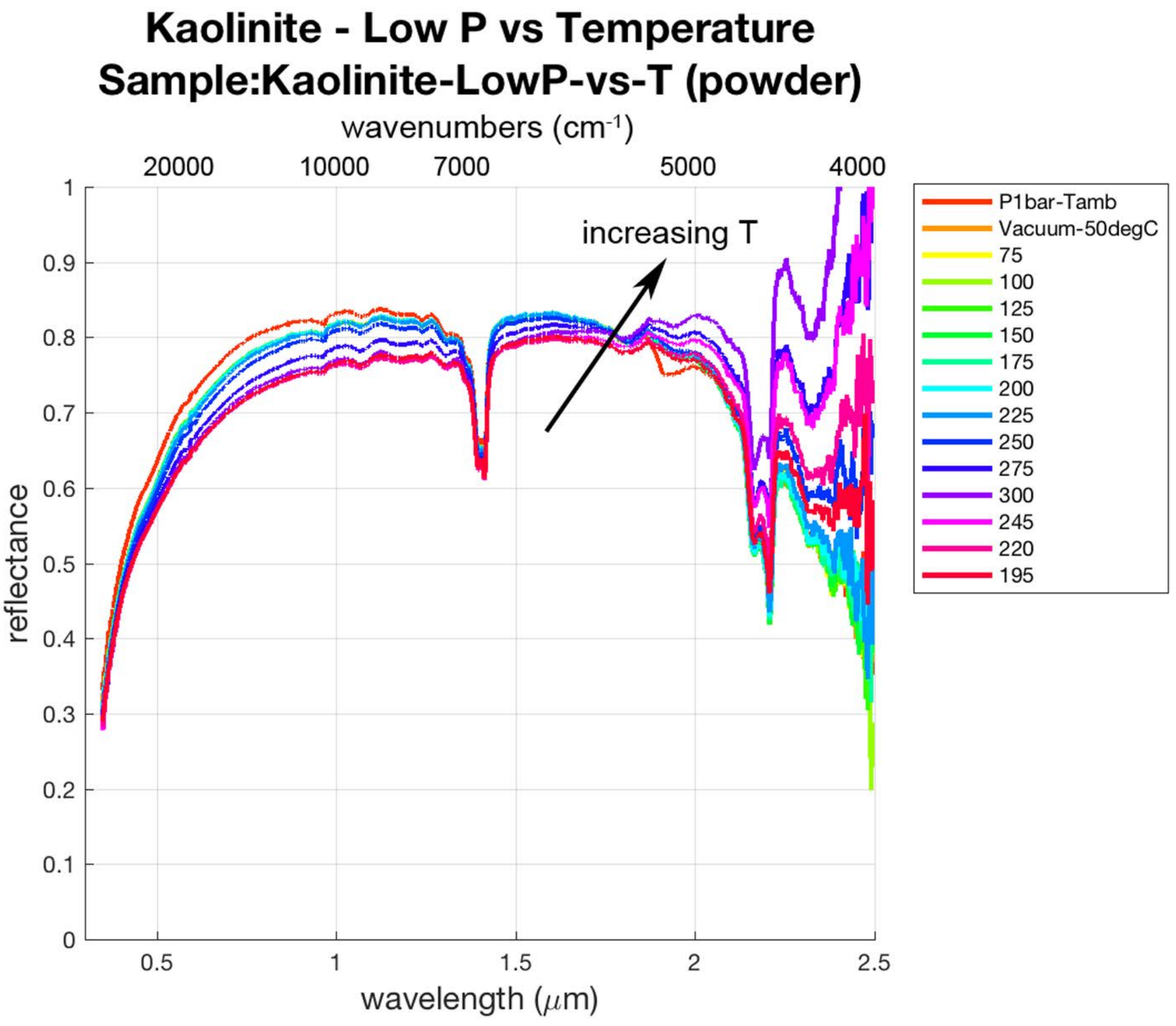
Kaolinite - Low P vs Temperature
Sample:Kaolinite-LowP-vs-T (powder)
wavenumbers (cm-1)
20000
10000
7000
5000
4000
increasing T
reflectance
wavelength (μm)
0
0.1
0.2
0.3
0.4
0.5
0.6
0.7
0.8
0.9
1
0.5
1
1.5
2
2.5
P1bar-Tamb
Vacuum-50degC
75
100
125
150
175
200
225
250
275
300
245
220
195

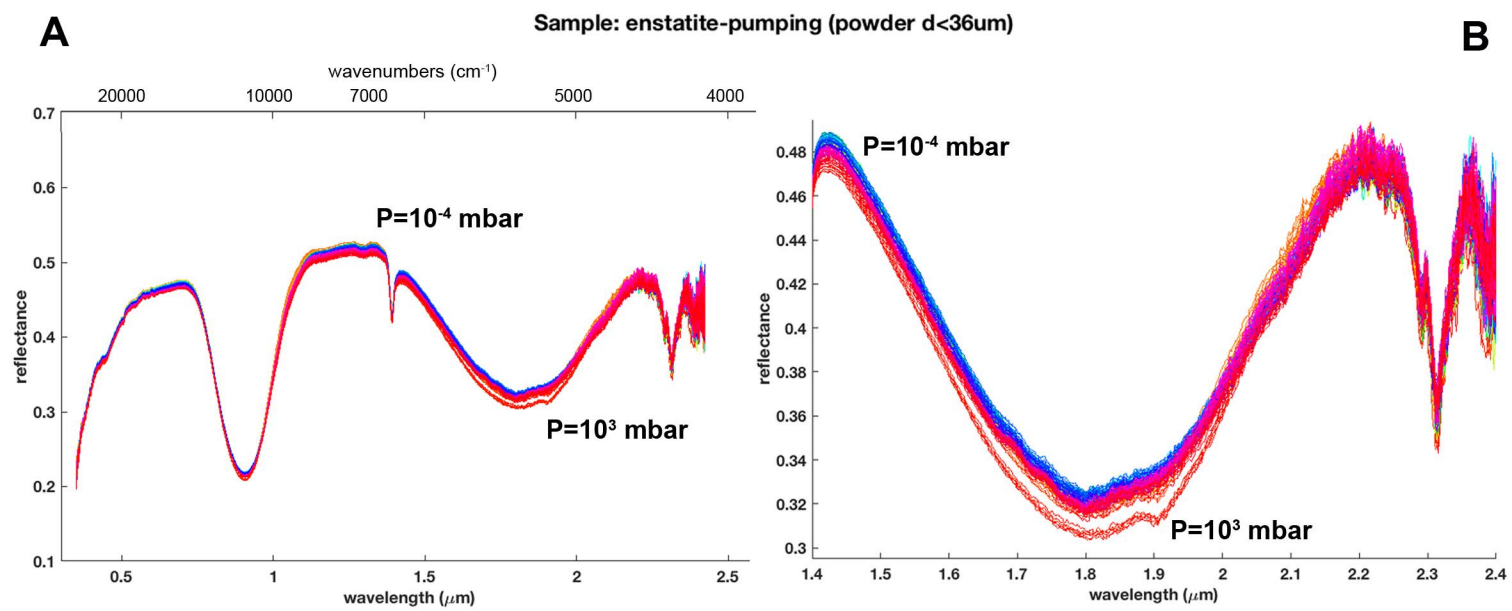
A
Sample: enstatite-pumping (powder d<36um)
B
wavenumbers (cm-1)
20000
10000
7000
5000
4000
P=10-4 mbar
P=103 mbar
reflectance
wavelength (μm)
0.7
0.6
0.5
0.4
0.3
0.2
0.1
0.5
1
1.5
2
2.5
0.48
0.46
0.44
0.42
0.4
0.38
0.36
0.34
0.32
0.3
1.4
1.5
1.6
1.7
1.8
1.9
2
2.1
2.2
2.3
2.4

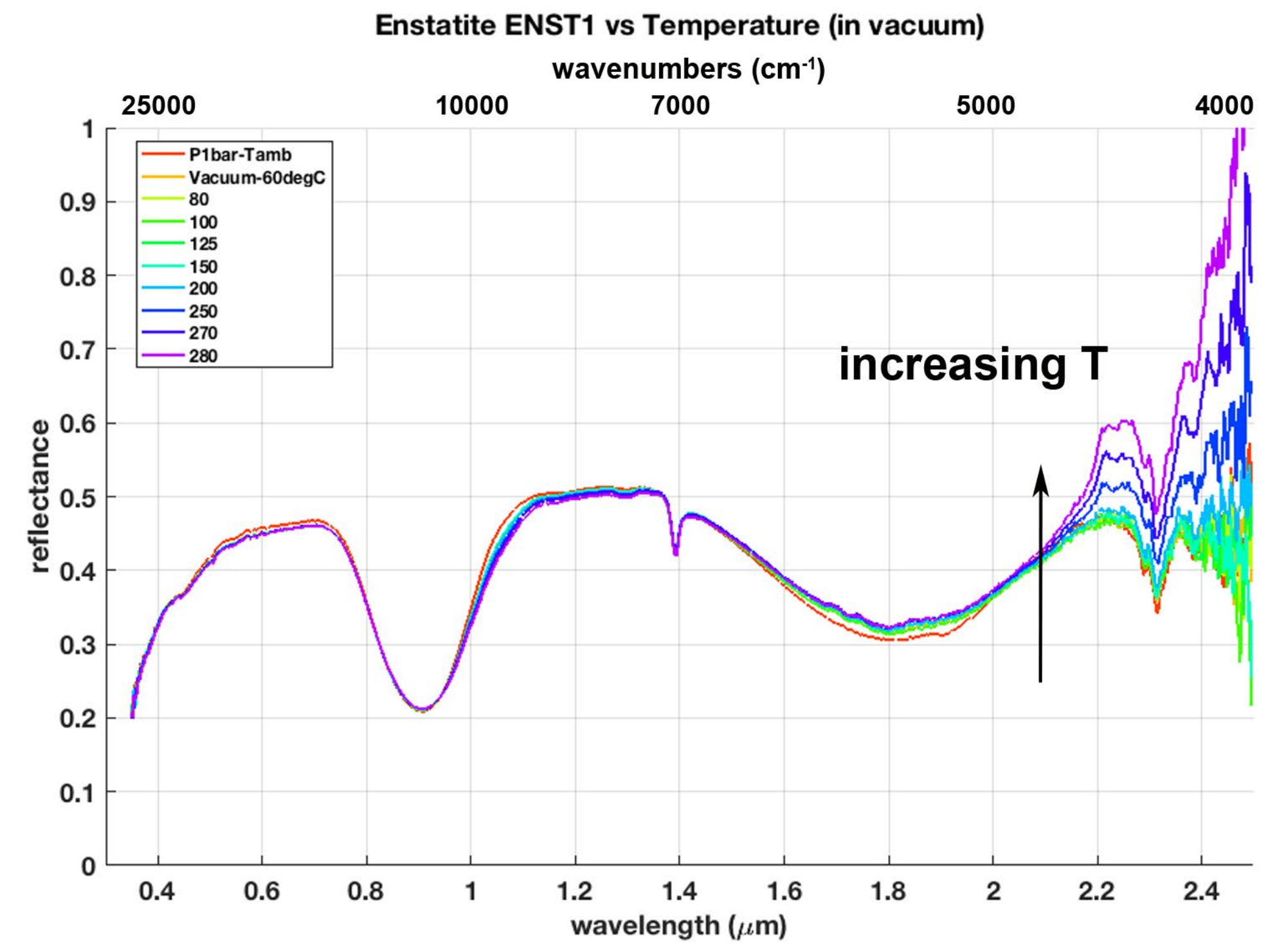
Enstatite ENST1 vs Temperature (in vacuum)
wavenumbers (cm-1)
25000
10000
7000
5000
4000
P1bar-Tamb
Vacuum-60degC
80
100
125
150
200
250
270
280
increasing T
reflectance
wavelength (μm)
0
0.1
0.2
0.3
0.4
0.5
0.6
0.7
0.8
0.9
1
0.4
0.6
0.8
1
1.2
1.4
1.6
1.8
2
2.2
2.4

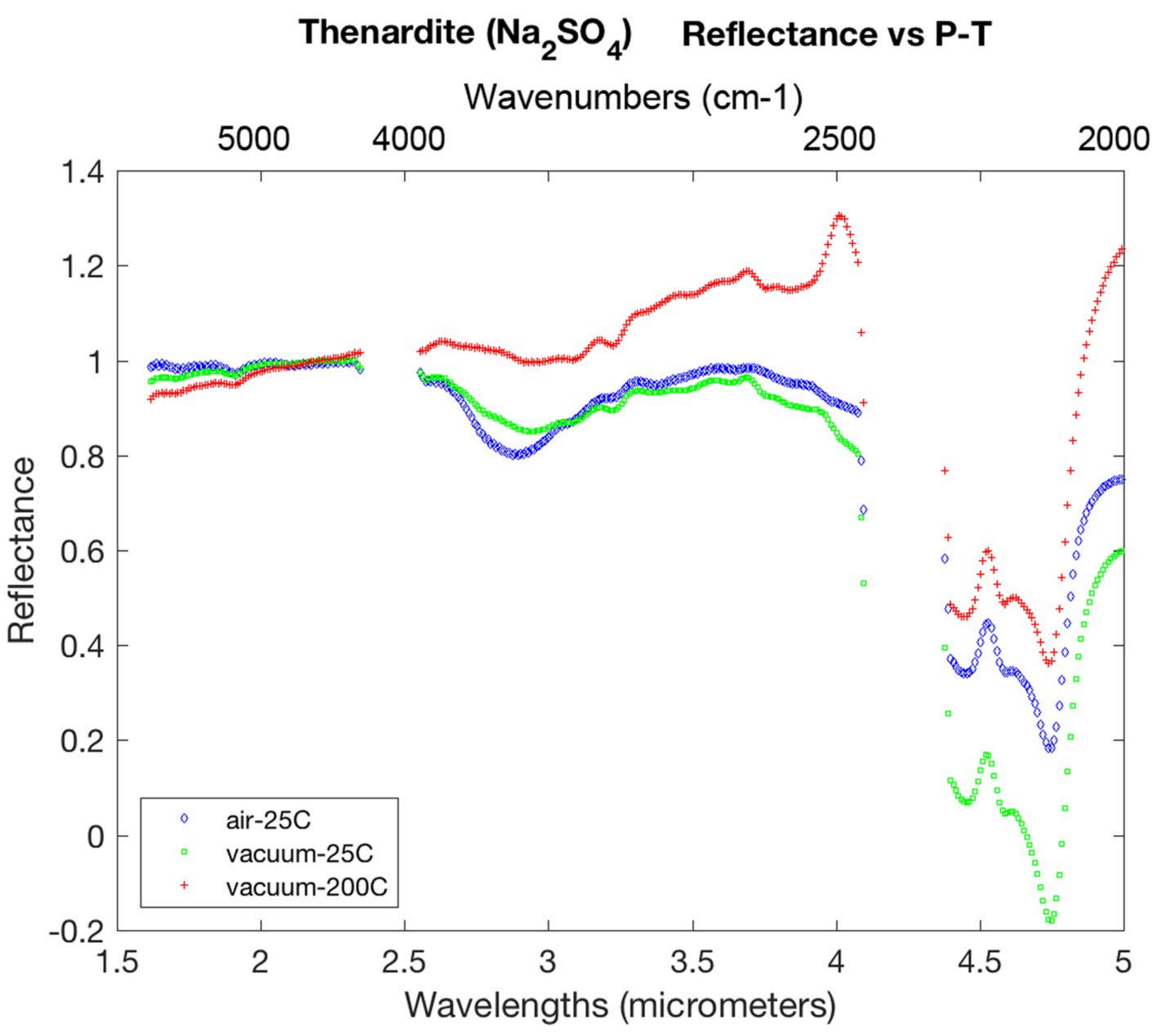
Thenardite (Na_2SO_4) Reflectance vs P-T
Wavenumbers (cm-1)
5000
4000
2500
2000
1.4
1.2
1
0.8
0.6
0.4
0.2
0
-0.2
Reflectance
air-25C
vacuum-25C
vacuum-200C
1.5
2
2.5
3
3.5
4
4.5
5
Wavelengths (micrometers)

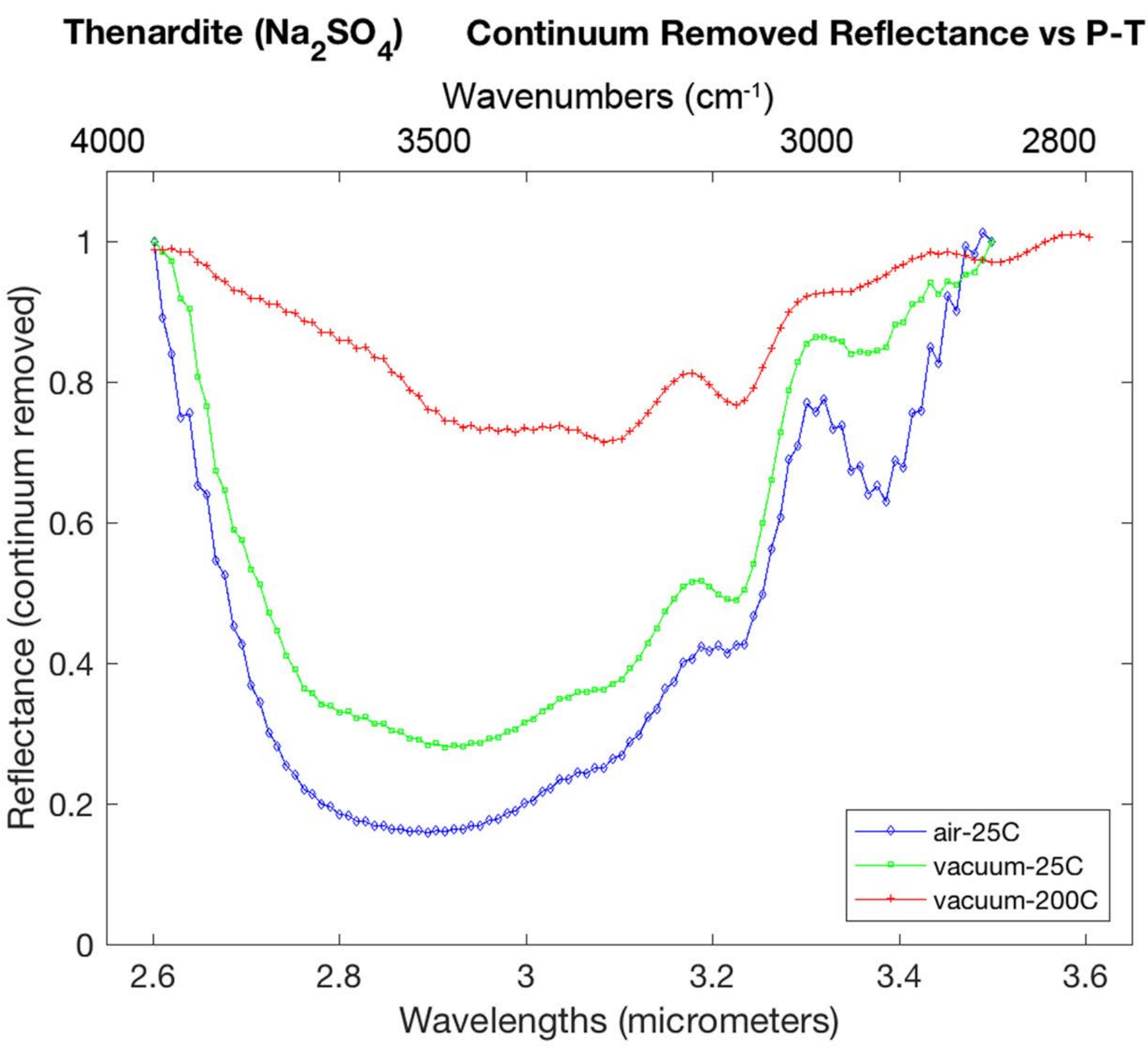
Thenardite (Na_2SO_4) Continuum Removed Reflectance vs P-T
Wavenumbers (cm^{-1})
4000
3500
3000
2800
Reflectance (continuum removed)
1
0.8
0.6
0.4
0.2
0
2.6
2.8
3
3.2
3.4
3.6
Wavelengths (micrometers)
air-25C
vacuum-25C
vacuum-200C